Sustainable Energy, Grids and Networks 36 (2023) 101184

Contents lists available at ScienceDirect

Sustainable Energy, Grids and Networks

journal homepage: www.elsevier.com/locate/segan

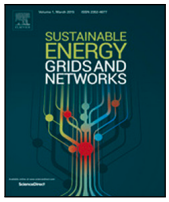

Robust opportunistic optimal energy management of a mixed microgrid under asymmetrical uncertainties

Amal Nammouchi [a,*], Phil Aupke [a], Fabio D'Andreagiovanni [b,c], Hakim Ghazzai [d], Andreas Theocharis [e], Andreas Kassler [a,f]

[a] Karlstad University, Computer Science Department, 65635 Karlstad, Sweden
[b] French National Centre for Scientific Research (CNRS), France
[c] Heudiasyc UMR 7253, Sorbonne Universités, Université, de Technologie de Compiègne, CNRS, CS 60319, 60203 Compiègne, France
[d] King Abdullah University of Science and Technology (KAUST), Thuwal, Saudi Arabia
[e] Karlstad University, Engineering and Physics Department, 65635 Karlstad, Sweden
[f] Deggendorf Institute of Technology, Faculty of Applied Computer Science, 94469 Deggendorf, Germany

ARTICLE INFO

Keywords:
Renewable energy
Robust optimization
Smart grid
Machine learning and AI

ABSTRACT

Energy management within microgrids under the presence of large number of renewables such as photovoltaics is complicated due to uncertainties involved. Randomness in energy production and consumption make both the prediction and optimality of exchanges challenging. In this paper, we evaluate the impact of uncertainties on optimality of different robust energy exchange strategies. To address the problem, we present AIROBE, a data-driven system that uses machine-learning-based predictions of energy supply and demand as input to calculate robust energy exchange schedules using a multiband robust optimization approach to protect from deviations. AIROBE allows the decision maker to tradeoff robustness with stability of the system and energy costs. Our evaluation shows, how AIROBE can deal effectively with asymmetric deviations and how better prediction methods can reduce both the operational cost while at the same time may lead to increased operational stability of the system.

1. Introduction

1.1. Background

Microgrids (MGs) [1,2] are small-scale power systems, consisting of interconnected loads and distributed energy resources (DERs). They have emerged as a promising solution to address the challenges of climate change and the rising electricity demand and offer several advantages. They provide localized energy generation, enhance grid resilience, promote renewable energy integration, and enable efficient energy management [3,4]. Energy management systems (EMSs) optimization and energy planning play vital roles in the effective operation of MGs [5]. By employing advanced modelling techniques and optimization algorithms, EMSs optimize the allocation and utilization of available energy resources within the microgrid. Energy planning ensures that energy generation, storage, and consumption are coordinated to maximize efficiency, minimize costs, and maintain grid stability [6].

However, renewable energy generation [7] and MGs loads are subject to inherent uncertainties. For example, fluctuations in weather conditions, such as varying solar radiation due to changes in clouds, precipitation, and wind speed, introduce volatility in renewable energy generation. Customer energy consumption behaviours vary on different timescales due to unpredictable personal behaviour or more long-term household size variations, weather conditions fluctuations that impact the heating and thus energy consumption or the addition of new electrical appliances and devices such as electric vehicles [8]. Such uncertainties make it difficult to predict renewable energy generation and consumption patterns precisely and may lead to large prediction errors.

Furthermore, these uncertainties can severely impact microgrid operations' resilience and cost-effectiveness, leading to supply–demand unbalance, compromising customer comfort, and imposing technical limitations on the system [9,10]. In this context, it is crucial to develop robust scheduling models that effectively address forecast uncertainty and better reflect the actual variation and different characteristics of the load and generation variations, including the asymmetry and

* Corresponding author.
E-mail addresses: amal.nammouchi@kau.se (A. Nammouchi), phil.aupke@kau.se (P. Aupke), d.andreagiovanni@hds.utc.fr (F. D'Andreagiovanni), hakim.ghazzai@kaust.edu.sa (H. Ghazzai), andreas.theocharis@kau.se (A. Theocharis), andreas.kassler@kau.se (A. Kassler).

https://doi.org/10.1016/j.segan.2023.101184
Received 21 February 2023; Received in revised form 3 August 2023; Accepted 30 September 2023
Available online 10 October 2023

List of Symbols

Variables

$b_{j,t}^{ch} \geq 0, \forall t \in T$	amount of charge of a user j's battery in period t, kW
$b_{j,t}^{dis} \geq 0, \forall t \in T$	amount of discharge of a user j's battery in period t, kW
$p_t^{exp} \geq 0, \forall t \in T$	amount of power exported in each period t, kW
$p_t^{imp} \geq 0, \forall t \in T$	amount of power imported in each period t, kW
$p_{j,t}^{PC}$	load of a user j' in period t, kW
$p_{j,t}^{PV}$	generated renewable power of a user j' in period t, kW
$SoE_{j,t} \geq 0, \forall t \in T$	state of energy of user j's battery in period t, kWh
$x_{j,t}^{ch} \in \{0,1\}, \forall j \in J, t \in T$	equal to 1 if the battery of user j is charged in period t and 0 otherwise
$x_{j,t}^{dis} \in \{0,1\}, \forall j \in J, t \in T$	equal to 1 if the battery of user j is discharged in period t and 0 otherwise
$y_t^{ex} \in \{0,1\}, \forall t \in T$	equal to 1 if power is exported by the MG in period t and 0 otherwise
$y_t^{im} \in \{0,1\}, \forall t \in T$	equal to 1 if power is imported by the MG in period t and 0 otherwise

Parameters

$\bar{p}_{j,t}^{PC}$	nominal (predicted) load of a user j' in period t, kW
$\bar{p}_{j,t}^{PV}$	nominal (predicted) generated renewable power of a user j' in period t, kW
Δt	duration of a time period t, hours
$\delta_{j,t}^{PC+}$	maximum load deviation of user j in period t, kW
$\delta_{j,t}^{PC-}$	minimum load deviation of user j in period t, kW
$\delta_{j,t}^{PV+}$	maximum PV power deviation of user j in period t, kW
$\delta_{j,t}^{PV-}$	minimum PV power deviation of user j in period t, kW
Γ_t^{PC}	budget of uncertainty for negative deviations of the MG load in period t
Γ_t^{PV}	budget of uncertainty for negative deviations of the MG PV power in period t
π_t^{ex}	revenue for export to the main grid at t
π_t^{im}	cost for import from the main grid at t
Θ_t^{PC}	budget of uncertainty for favourable deviations of the MG load in period t
Θ_t^{PV}	budget of uncertainty for favourable deviations of the MG PV power in period t
Exp_t	maximum exported power at t, kW
Imp_t	maximum imported power at t, kW
J	maximum level of protection
k_j^{ch}	maximum charging power of user j at t, kW
k_j^{dis}	maximum discharging power of user j at t, kW
SoE_j^{max}	upper bound of $SoE_{j,t}$, kWh
SoE_j^{min}	lower bound of $SoE_{j,t}$, kWh

Indices and Sets

$j \in C$	Index of a user and set the users in a MG
$t \in T$	Index and set of time steps (hours)

variability nature of prediction errors. By adequately addressing these uncertainties, MGs operators can make informed decisions and implement effective sustainable and reliable energy supply strategies.

1.2. Literature review

Optimal control is extensively used to determine the MGs operations. In this context, several studies have explored deterministic approaches to optimize the EMS in MGs. In [11], the authors propose MILP solution approach that optimizes the MG operation with respect to on/off connection status of main grid, fuel cell, and energy storage system (ESS). In [12], the authors proposed a techno-economic MILP based optimization model to compute the load scheduling in MG EMS. More studies proposed deterministic approaches to schedule the EMS operations [13–16] while assuming perfect knowledge about the future without protecting against any forecast errors. Extensive literature review on more optimal control strategies can be found in [17]. In contrast to optimal control based approaches, our work AIROBE is robust as it protects from forecast errors.

The growing prevalence of renewable energy and random behaviour of the customers has brought about significant uncertainty in MGs. The current literature frequently employs various methods to address this uncertainty, including stochastic optimization (SO), chance-constrained optimization (CCO), meta-heuristic approaches, data-driven deep reinforcement learning (DRL), and robust optimization (RO).

Stochastic frameworks, which require knowledge about the probability distributions to describe the uncertainty are traditionally used for uncertainty modelling [26–28]. In [29], the authors present an energy scheduling strategy of the MG operation based on the probabilistic forecasts of both the wind power and the user's demand. The authors in [30] propose a stochastic optimization framework for smart home energy management while considering the uncertainty associated with the DERs generation and the plug-in electric vehicle's plug-state. A genetic algorithm (GA) based EMS was introduced in [31] to achieve optimal generation and reserve scheduling for a grid-connected MG. The approach considers uncertainties associated with wind power and load demand through scenario generation and reduction techniques. In scenario-based SO, a set of potential future scenarios is generated by considering the known characteristics of uncertain variables. These scenarios are then reduced to a more manageable size, and a robust optimization process under the worst-case scenario is conducted.

In [32], the authors formulate a chance-constrained optimization (CCO) problem for the optimal scheduling of a MG with islanding capability, which is then solved by a MILP. The formulation takes into account the probability distributions of forecast errors of wind, PV and load. In [33], the authors propose two EMS models for peak shaving and system protection, and frequency regulation, respectively, in a centralized manner. The authors handle the uncertainty using probabilistic constraints.

Meta-heuristic based approaches are often used to speed the solving process and improve the scalability. In [34], the authors use Particle swarm optimization (PSO) to handle the MG operation, emission and costs. Beta and Weibull probability density functions are used in point estimate method to model the uncertainties of solar power and wind power, respectively. Similarly, the authors in [34] develop an optimal EMS for a grid-connected MG under uncertainties of RERs, load demand, and electricity price. The uncertainties are modelled using point estimate method. The efficiency of PSO in finding best solution is shown to be better in comparison with GA, combinatorial PSO, fuzzy self-adaptive PSO, and adaptive modified PSO.

Table 1
MG control strategies from literature in comparison with AIROBE.

Ref	Control strategy	Uncertain RE	Uncertain load	Uncertain prices	Uncertainty range	Symmetry of the uncertainty range	Conservatism	Positive deviation
[18]	RO	Yes	No	Yes	Fixed +/−10% RE, +/−5% Pr	Symm	Worst case	No
[19]	Scenario-based RO	Yes	Yes	No	interval prediction method	Symm	Worst case	No
[20]	Two-stage RO	Yes	Yes	No	depends on previous slot	Symm	Worst case	No
[21]	Min–max Budgeted RO	Yes	Yes	No	Monte Carlo based samples	Symm	Budgeted worst case	No
[22]	Minimax Multi-obj RO	Yes	Yes	No	Polyhedral set	Symm	Point based minmax	No
[23]	Two-stage RO	Yes	No	No	Fixed +/−10% WT, +/−5% PV	Symm	Worst case	No
[24]	Budgeted RO	Yes	No	Yes	Fixed +/−25% RE, +/−20% Pr	Symm	Budgeted worst case	No
[25]	Quad. min–max RO	Yes	Yes	No	Fixed +/−10%	Symm	Budgeted worst case	No
AIROBE	Mod. Budgeted RO	Yes	Yes	No	Time-Varying based on forcast	Asymm	Flexible	Yes

Data-driven deep reinforcement learning (DRL) has recently been explored in the context of EMS as it helps to optimize the EMS in a distributed, secure manner while not relying on a specific probability distribution model of the environment to handle uncertainty [35]. For example, the authors in [36] use the DQN algorithm under uncertainties to solve wind farm management with energy storage. In [37], the authors propose a DRL-based DDPG algorithm to realize EMS dynamic energy dispatch, while in [37], DDPG is used to find the optimal control strategy of the battery in a MG. The authors in [38] suggested a decentralized framework based on hierarchical multi-agent reinforcement learning under uncertainty to solve the resilience-driven dispatch problem of Mobile power sources MPSs and repair crews (RCs) in MGs. However, research in this field is still in the early stages, where the effectiveness of learning relies on the selection of hyperparameters. The generalization to new environments is still an ongoing research challenge, and further studies are needed.

Robust optimization (RO) has been extensively used, as an alternative to scenario-based approaches as it has better computational performance and simpler uncertainty modelling [39]. RO methods that consider the worst-case scenario is utilized frequently in this context [18–20,23]. In worst-case scenario-based approach, the uncertain parameters are assumed to take on their worst possible values. However, both the positive and negative errors exist in the uncertainty as shown in Section 2. In this study, we focus on developing an opportunistic RO based method that reflects better the characteristics of the uncertainty ranges. We summarize the relevant literature and compare them to AIROBE, the proposed model in Table 1.

The authors in [24] investigate the energy management in MGs in relation with the uncertainty derived from the energy price signals, which deviate within a fixed symmetrical uncertainty range equal to ±20 for all time periods. Similar assumptions about the uncertainty ranges (fixed and symmetrical) were adopted in the following studies [18,23,25], which differs from our work that focuses on the uncertainty on the PV generation and the load side, given a budget of uncertainty under asymmetrical deviations. In recent work of [25], the authors presented a quadratic min–max robust solution under the cardinality-constrained uncertainty set based on the classical Gamma robustness theory [39] for energy management of a residential MG under uncertainties on demand and renewable power generation. The proposed solution protects against the worst-case scenario, based on symmetric deviation ranges with fixed uncertainty. Similarly, in [40] the authors propose robust energy scheduling solution for a smart building under PV generation uncertainty. The authors also use the budget of uncertainty based model and consider PV output forecasting as an input, and they assume that the upper and lower bounds deviate 20% from the forecasted values. In contrast, our work introduces favourable deviations and incorporates time-varying and asymmetrical uncertainty ranges.

1.3. Contributions

In order to address the issue of reliable and cost efficient scheduling, we propose in this paper AIROBE, which is a data-driven optimization model that protects against time-varying asymmetric deviations of predicted load and PV power generation. The goal from this work is to use machine-learning (ML)-based predictions as input to a less conservative robust optimization approach that accounts for both asymmetrical good (positive errors) and bad (negative errors) deviations instead of the absolute worst case, in opposition to the classical RO approaches. The specific contributions of this paper are as follows:

1. We propose a tractable and comprehensive robust model to solve the optimal energy scheduling problem of a grid-connected mixed MG (residential and non residential users). The robust model accounts for the dynamicity of the energy prices and the uncertainties yielded from the PV generation and users' consumption profiles.
2. We use variable uncertainty ranges for both the load and the PV generation that are computed with ML based forecast, for each time slot. The forecasting is based on pre-clustering method that clusters the data into sunny, rainy, overcast, and partial overcast days. The deviation ranges are strongly affected by this clustering, and impacts the energy scheduling and optimization.
3. We propose a refined robust optimization approach for MGs scheduling under asymmetric load and PV generation uncertainties. In contrast to classical robustness model, the proposed robust model allows to take into account bad and good deviations over asymmetrical intervals, allowing to obtain less conservative solution without sacrificing protection against uncertainty.
4. The proposed solution is validated via simulations using real-world data set and evaluated using the price of robustness and the probability of the constraint violation in order to decide the trade-off between the cost and the energy balance violation. We demonstrate that our approach reduces the conservatism of the MG operation and decreases the MGs cost without impacting the constraint violation probability in comparison with the original budget-of-uncertainty model [39].

The remainder of this paper is organized as follows. Section 2 motivates our work and the proposed robust formulation. Section 3 presents our robust mathematical formulation. In Section 4, we describe our ML-based forecasting models that predict uncertainty ranges as input for the model. In Section 5, we perform several case studies where we compare our approach with RO baselines. In Section 6, we discuss how the proposed solution can help the decision makers take better decisions, and we delve into the model limitations and future work. We conclude the article in 7.

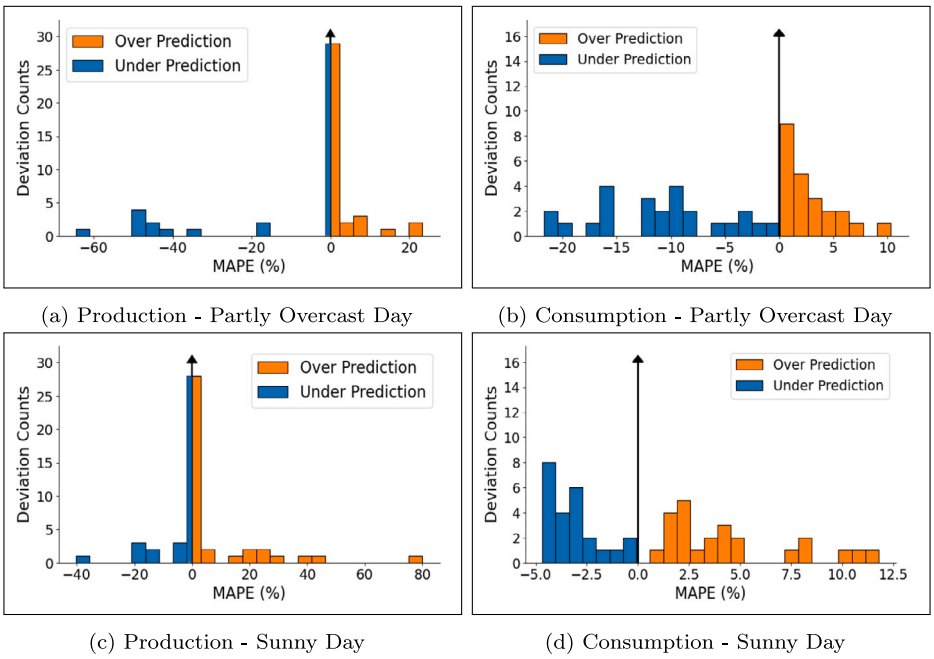

(a) Production - Partly Overcast Day (b) Consumption - Partly Overcast Day

(c) Production - Sunny Day (d) Consumption - Sunny Day

Fig. 1. Distribution of over- and under-prediction in terms of MAPE for one prosumer for PV power generation ((a) and (c)) and energy consumption ((b) and (d))during 24 h (for a partly overcast and a sunny day).

2. Motivation

In this section, we characterize forecast errors for MG load and RE generation predictions. Such predictions are needed for optimizing the energy scheduling in smart MGs. We illustrate different types of prediction errors that may occur. Finally, we describe research challenges when developing robust but opportunistic MG power scheduling methods under the presence of such forecast errors.

2.1. Uncertainties in MG load and generation forecasts

The optimization of energy exchanges in smart MGs is impacted by different uncertainties that arise when predicting power production of renewables and energy consumption of the prosumer in the system. In order to illustrate typical forecast errors, we trained different ML-based forecast models to predict PV production and energy consumption. Our models use clustering techniques and consider the weather characteristics in order to increase model accuracy as explained in Section 4. Fig. 1 illustrates different distributions of the forecasting Mean Absolute Percentage Error (MAPE) when predicting the PV power generation (Fig. 1(a,c)) and energy consumption (Fig. 1(b,d)). We plot the results for two clusters, i.e, sunny and partly overcast. The blue sections of the histogram represent under-prediction, where the forecasted values are lower than the actual measured ones. The orange sections show over-prediction, where the predicted value is larger than the actual value. Fig. 2 illustrates the variability of the deviation for the production and consumption prediction over time with a confidence interval (CI) of 80%.

We summarize our main findings as follows:

- **Different weather conditions result in different error characteristics:** the deviations of observed values from predicted ones in terms of under- and over predictions behave differently for each of the weather conditions (see Fig. 1). For example, when observing the prediction error for PV production and consumption for the partly overcast days, we notice a trend for larger negative deviation of the observed values from the predicted values leading to higher under prediction. However, for sunny days, there is a trend towards over prediction of both energy supply and demand.
- **Asymmetrical deviation:** the deviation, i.e., the difference between predicted value and observed value of the PV production and the prosumer consumption is asymmetrical, i.e, the lower and the upper bounds of the deviations are not equal as shown in Fig. 1.
- **Uncertainty varies over different prediction horizons:** Fig. 2 plots deviations of predicted values from observed values for both PV production and energy consumption of a single prosumer over a whole day. As can be seen, the deviation range and asymmetry varies over different time-slots.

2.2. Research challenges

Based on these observations, we conclude that the MGs operation may be severely impacted by asymmetric time-varying deviations caused by the uncertainties involved when forecasting both the PV power generation and the prosumers consumption. Given these uncertainties, the MGs scheduling problem can be categorized as an optimization problem with resource uncertainty, where the predicted consumption and production have uncertain upper and lower bounds for each time slot. Due to these deviations, the worst-case scenario happens when the realized PV power generation is lower than expected, or alternatively, when the consumption is higher than predicted. These deviations can be described as bad deviations for our system.

As illustrated in Fig. 1, both positive and negative forecast errors contribute to the uncertainty. In fact, the true available PV power may be much higher than the predicted value (i.e., under under-prediction of the generated power) and the consumption can be lower than expected (i.e., under over-prediction of the energy consumption). In this case, using a worst-case scenario-based scheduling using predicted values results in a schedule where the total available power may never be entirely utilized by the MGs. Consequently, the planned decisions are overly conservative and may also entail high costs. These deviations can be described as good deviations in our system, as such situation results in energy surplus which our model aims to exploit. It is important to note that because RO conservatism, the optimization results of uncertainty variables representing prediction errors tend to be in the same direction, i.e, the negative direction.

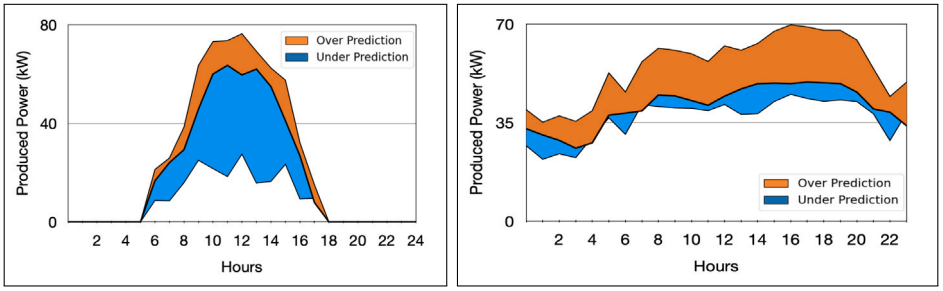

(a) Asymmetrical Deviation - PV Power Production (b) Asymmetrical Deviation - Energy Consumption

Fig. 2. Deviations for one prosumer PV power generation (a) and energy consumption (b) during 24 h.

In fact, if the MGs scheduling is planned solely based on predicted values, even small prediction errors and uncertainties associated with the demand and the available power can make the planned power dispatch infeasible, potentially lead to high operational costs (e.g., due to unplanned high demand or low supply), and may lead to security and reliability issues in the power system when using the predicted values for the MGs operation in real-time.

Furthermore, Fig. 2 illustrates, that the deviation of a day-ahead prediction is variable over time and is not constant or symmetrical as developed in the literature. Hence, our proposed approach must be able to optimize the MGs energy scheduling under time-varying and asymmetric deviations.

2.3. Solution approach

As a consequence, we need to formulate our model so that it protects against the bad deviations and reduces unnecessary protection by taking advantage of the good deviations in an opportunistic less conservative manner. Our approach proposes a more accurate uncertainty quantification method using ML, and then integrate the output into a reformulation of RO based method that reflects better the uncertainty characteristics including: asymmetry of uncertainty ranges, variability of uncertainty ranges over time, and different amounts of positive and negative forecast errors.

3. Modelling the MG energy exchange optimization problem

We consider a MG made up of a cluster of prosumers and consumers that are geographically close. Each prosumer is equipped with a battery, a PV cell, and is associated with a power load. Each consumer is associated with a power load. It is not equipped with a PV cell but may possess a battery (e.g., for electric vehicles or load coverage). The prosumers and consumers can exchange power (import/export, i.e., buy/sell) among each other, and the MG can exchange power with the main grid to cover its demand or to sell its surplus. The prices of power imports and exports are dynamic (i.e., they may vary over the time periods constituting the planning horizon that we consider).

Given a time horizon decomposed into a set of time periods T and given an MG including a set C of users (prosumers or consumers), the optimal MG exchange problem that we consider is that of choosing the charge/discharge actions of each user and import/export actions of the MG in each time period, satisfying the total MG load constraint while taking into account the PV generation and the state-of-the-energy constraints, with the aim of minimizing the total cost of the MG over the horizon. In this work, we assume that battery degradation and leakage effects are negligible.

3.1. Deterministic optimization model

We start by defining the deterministic model, which does not take into account the uncertainty of users' loads and PV generation. The different parameters and decision variables are summarized in the list of symbols.

These decision variables are employed in a number of constraints. First, we must express the link between the charge (discharge) binary and continuous variables, imposing that the continuous charge (discharge) variables of a user $j \in C$ in period $t \in T$ cannot exceed an upper bound k_j^{ch} (k_j^{dis}) when a charge (discharge) occurs in a period:

$$b_{j,t}^{ch} \leq k_j^{ch} \cdot x_{j,t}^{ch} \qquad \forall j \in C, t \in T, \tag{1}$$

$$b_{j,t}^{dis} \leq k_j^{dis} \cdot x_{j,t}^{dis} \qquad \forall j \in C, t \in T. \tag{2}$$

Furthermore, we must express that a user j can either charge or discharge its battery in each period t, i.e.:

$$x_{j,t}^{ch} + x_{j,t}^{dis} \leq 1 \qquad \forall j \in C, t \in T. \tag{3}$$

Similarly, we must express the variable upper bound Imp_t (Exp_t) on the power that may be imported (exported) in each time period $t \in T$ and the condition of either importing or exporting in each period, i.e.:

$$p_t^{im} \leq \mathrm{Imp}_t \cdot y_t^{imp} \qquad \forall t \in T, \tag{4}$$

$$y_t^{im} \leq Exp_t \cdot y_t^{exp} \qquad \forall t \in T, \tag{5}$$

$$y_t^{im} + y_t^{ex} \leq 1 \qquad \forall t \in T. \tag{6}$$

We also include constraints on the State of Energy (SoE), linking the value of SoE variables to the energy variation occurring between consecutive time periods (here Δt is the duration of a time period) and imposing bounds SoE_j^{min}, SoE_j^{max} on the minimum and maximum values that an SoE variable may assume:

$$SoE_{j,t} = SoE_{j,t-1} + (b_{j,t-1}^{ch} - b_{j,t-1}^{dis}) \cdot \Delta t \qquad \forall j \in C, t \in T, \tag{7}$$

$$SoE_j^{min} \leq SoE_{j,t} \leq SoE_j^{max} \qquad \forall j \in C, t \in T. \tag{8}$$

Eventually, we define the load constraints imposing that, for each period $t \in T$, the sum of the power $p_{j,t}^{PV}$ produced through PV by each user $j \in J$ plus the sum of the charge/discharge variation of batteries of all users and the import/export variation with the main grid must be greater or equal than the sum of the load $p_{j,t}^{PC}$ of the users, i.e.:

$$\sum_{j \in C} \left[p_{j,t}^{PV} + \left(b_{j,t}^{dis} - b_{j,t}^{ch} \right) \right] + \left(p_t^{imp} - p_t^{exp} \right) \geq \sum_{j \in C} p_{j,t}^{PC} \qquad \forall t \in T. \tag{9}$$

The objective is to minimize the total cost of power import/export over the entire time horizon, obtained by summing the difference between the cost of importing (with price π_t^{im}) and the revenue of exporting (with price π_t^{ex}):

$$\min \sum_{t \in T} (\pi_t^{im} \cdot p_t^{im} - \pi_t^{ex} \cdot p_t^{ex}). \tag{10}$$

3.2. Robust optimization model

The previous model is deterministic and neglects the fact that both the load coefficients $p_{j,t}^{PC}$ and PV power generation coefficients $p_{j,t}^{PV}$

of constraints (9) are subject to uncertainty and their exact value is not known in advance. In order to tackle such data uncertainty, which may lead to infeasibility and severe suboptimality of solutions when neglected and not properly taken into account in the model (see [41] for an exhaustive discussion), we propose to adopt a Robust Optimization (RO) approach. RO is a methodology that takes into account data uncertainty under the form of hard constraints that are added to the model for considering only *robust solutions*, namely solutions whose feasibility is preserved even when data deviations specified by an uncertainty set occur.

We start by considering a classical RO model, so called Γ-Robustness [39], then we propose an improved RO model that allows to more accurately represent data deviations. In a more formal way, in an RO approach: (1) the *actual value* of an uncertain coefficient is supposed to equal the summation of a reference value *nominal value* set by the decision maker and an unknown deviation; (2) an *uncertainty set* is defined for specifying all possible deviations for which protection is required; (3) it is defined a *robust counterpart*, namely a modified version of the original deterministic optimization problem that includes only robust solutions. Granting robustness comes at the so-called *price of robustness*, which is a degradation in the optimal value caused by excluding non-robust solutions from the feasible set. In general, increasing robustness and thus adding protection against uncertainty leads to a higher price of robustness.

In the optimization model presented in Section 3.1, the uncertainty affects the load–supply constraints (9): following the Γ-Robustness approach, we assume that the actual value of each uncertain load coefficient $p^{PC}_{j,t}$ and of each PV power generation coefficient $p^{PV}_{j,t}$ falls in the symmetric intervals:

$$p^{PV}_{j,t} \in [\bar{p}^{PV}_{j,t} - \delta^{PV}_{j,t}, \bar{p}^{PV}_{j,t} + \delta^{PV}_{j,t}]$$
$$p^{PC}_{j,t} \in [\bar{p}^{PC}_{j,t} - \delta^{PC}_{j,t}, \bar{p}^{PC}_{j,t} + \delta^{PC}_{j,t}] \quad (11)$$

where $\bar{p}^{PV}_{j,t}$, $\bar{p}^{PC}_{j,t}$ are the nominal values and $\delta^{PV}_{j,t}, \delta^{PC}_{j,t}$ the corresponding maximum deviation. Furthermore, the approach provides for introducing parameters $\Gamma^{PV}_t \in \{0, |J|\}$, $\Gamma^{PC}_t \in \{0, |J|\}$ denoting the number of load and PV generation coefficient deviations for which protection is requested in each period $t \in T$. These parameters represent a budget of uncertainty and allow to control the level of protection against uncertainty and the corresponding price of robustness: when $\Gamma_t = 0$ no protection is imposed and the price of robustness is null; by increasing the value of Γ_t, the protection and the price of robustness increase, until reaching full protection for $\Gamma_t = |J|$, which also entails the highest price of robustness.

Using the theoretical results of Γ-Robustness presented in [39], we can write the following robust counterpart of the constraints (9):

$$\sum_{j\in C}\left[\bar{p}^{PV}_{j,t} + \left(b^{dis}_{j,t} - b^{ch}_{j,t}\right)\right] - \left(\Gamma^{PV}_t \cdot v^{PV}_t + \sum_{j\in C} w^{PV}_{j,t}\right) + \left(p^{imp}_t - p^{exp}_t\right)$$
$$\geq \sum_{j\in C}\bar{p}^{PC}_{j,t} + \left(\Gamma^{PC}_t \cdot v^{PC}_t + \sum_{j\in C} w^{PC}_{j,t}\right) \qquad \forall t \in T, \quad (12)$$

$$v^{PV}_t + w^{PV}_{j,t} \geq \delta^{PV}_{j,t} \qquad \forall j \in C, t \in T, \quad (13)$$
$$v^{PC}_t + w^{PC}_{j,t} \geq \delta^{PC}_{j,t} \qquad \forall j \in C, t \in T, \quad (14)$$
$$v^{PV}_t,\ v^{PC}_t \geq 0 \qquad \forall t \in T, \quad (15)$$
$$w^{PV}_{j,t}, w^{PC}_{j,t} \geq 0 \qquad \forall j \in C, t \in T. \quad (16)$$

which is made up of: (i) the robust constraint (12), which is a modified version of (9) that refers to the nominal coefficient values $\bar{p}^{PV}_{j,t}$, $\bar{p}^{PC}_{j,t}$ and includes additional terms modelling the deviations of coefficients and the Γ parameters controlling robustness; (ii) auxiliary constraints (13), (14) and auxiliary variables (15), (16) introduced by the procedure of [39] exploiting duality theory of Linear Programming.

3.3. A refined robust model considering asymmetrical and "good" deviations

While Γ-Robustness constitutes the most successful method for Robust Optimization and still represents a major reference that is widely used in a vast number of real-world uncertain optimization problems (see e.g, [41]), it offers opportunities for improvements. Here, we attempt at obtaining a more refined representation of uncertainty, reducing the price of robustness without sacrificing protection, by considering an asymmetrical range of deviation of the coefficients and taking into account "good" deviations in the value of coefficients. By "good" deviations, we intend favourable deviations in the value of coefficients, like an increase in the PV power production $p^{PV}_{j,t}$ or a reduction in the load $p^{PC}_{j,t}$, which strengthen feasibility instead of leading towards infeasibility: these deviations are indeed likely in reality, but are completely neglected by Γ-Robustness, which considers only worst-case "bad" deviations leading towards infeasibility.

As first step, we define the following modified deviation ranges:

$$p^{PV}_{j,t} \in [\bar{p}^{PV}_{j,t} - \delta^{PV-}_{j,t}, \bar{p}^{PV}_{j,t} + \delta^{PV+}_{j,t}]$$
$$p^{PC}_{j,t} \in [\bar{p}^{PC}_{j,t} - \delta^{PC-}_{j,t}, \bar{p}^{PC}_{j,t} + \delta^{PC+}_{j,t}] \quad (17)$$

in which the range is asymmetrical and the value of the largest negative deviations $\delta^{PV-}_{j,t}, \delta^{PC-}_{j,t}$ and positive deviations $\delta^{PV+}_{j,t}$ $\delta^{PC+}_{j,t}$ do not have to coincide, as common in real-world optimization under uncertainty [42].

The classical Γ-robust model is able to take into account only the "bad" deviations $\delta^{PV-}_{j,t}$ (decrease in the PV generation) and $\delta^{PC+}_{j,t}$ (increase in the load) and leads towards the infeasibility of the load constraint (9). If we want to take into account the "good" deviations $\delta^{PV+}_{j,t}$ (increase in the PV production) and $\delta^{PC-}_{j,t}$ (decrease in the load), it is necessary to extend the Γ-robust model, in particular introducing an additional parameter Θ_t specifying the minimum number of deviations that must be "good" and suitable associated constraints.

When considering the "good" deviations together with the "bad" deviations, we can prove the following results:

Proposition 1. *For each time period $t \in T$, the robust counterpart of constraint (9) when protection for Γ^{PV}_t "bad" deviations and Θ^{PV}_t "good" deviations of PV generation coefficients and Γ^{PC}_t "bad" deviations and Θ^{PC}_t "good" deviations of load coefficients are allowed in period t writes as:*

$$\sum_{j\in C}\left[\bar{p}^{PV}_{j,t} + \left(b^{dis}_{j,t} - b^{ch}_{j,t}\right)\right] - \left(\Gamma^{PV}_t \cdot v^{PV-}_t - \Theta^{PV}_t \cdot v^{PV+}_t + \sum_{j\in C} w^{PV}_{j,t}\right)$$
$$+ \left(p^{imp}_t - p^{exp}_t\right) \geq \sum_{j\in C}\bar{p}^{PC}_{j,t} + \left(\Gamma^{PC}_t \cdot v^{PC+}_t - \Theta^{PC}_t \cdot v^{PC-}_t + \sum_{j\in C} w^{PC}_{j,t}\right) \quad (18)$$

$$v^{PV-}_t + w^{PV}_{j,t} \geq \delta^{PV-}_{j,t} \qquad \forall j \in C \quad (19)$$
$$-v^{PV+}_t + w^{PV}_{j,t} \geq -\delta^{PV+}_{j,t} \qquad \forall j \in C \quad (20)$$
$$v^{PC+}_t + w^{PC}_{j,t} \geq \delta^{PC+}_{j,t} \qquad \forall j \in C \quad (21)$$
$$-v^{PC-}_t + w^{PC}_{j,t} \geq -\delta^{PC-}_{j,t} \qquad \forall j \in C \quad (22)$$
$$v^{PV+}_t,\ v^{PV-}_t \geq 0 \quad (23)$$
$$w^{PV}_{j,t} \geq 0 \qquad \forall j \in C \quad (24)$$
$$v^{PC+}_t,\ v^{PC-}_t \geq 0 \quad (25)$$
$$w^{PC}_{j,t} \geq 0 \qquad \forall j \in C \quad (26)$$

Proof. For the proof, we refer the reader to Appendix. □

4. Prediction of PV energy supply and demand

AIROBE requires as input the prediction of PV Energy Supply and Demand as well as its deviation ranges for each forecast interval. We

use data-driven approaches for obtaining model input as described below.

Data pre-processing. AIROBE integrates data cleaning techniques to improve data quality for making predictions of high quality. To detect outliers and missing data we are using interquartile range (IQR) method. Data points, which are not within a percentile of the mean are detected as outliers and replaced by the average of previous/future values. For the solar PV production, we also remove the night times, since they are not relevant for the prediction of solar energy production [43].

Weather type clustering. Previous work in this field has shown, that four clusters for the weather types (sunny, partly overcast, overcast and rainy) perform the best [44]. We cluster the data using the weather features available in the dataset (solar irradiation, temperature and humidity for the whole year) using K-means clustering in combination with dynamic time warping (DTW) to create the clusters. DTW has shown superior performance when applied to time-series datasets, because it is able to detect similar patterns even if they do not occur in the same time period [45].

Forecasting Models. We enrich the clustered datasets with the historical information about the PV power production and energy consumption of the prosumer in the system. For each of the four clusters we then generate an individual machine learning forecast model. As a predictor we use LightGBM, which is a gradient boosting decision tree (GBDT) algorithm [46]. LightGBM is constructed differently than conventional GBDT algorithms, as it grows leaf-wise to find a leaf with the largest split gain instead of iterating over all previous leaves. To additionally speed up the training of the model it uses advanced networking communication called parallel voting decision tree algorithm, which enables parallel computation during the training process [47,48]. Since the LightGBM regressor only supports single-step forecasting, we additionally wrapped an auto-regressive direct multi-step forecaster [49], which generates the multi-step forecast in a sliding window manner. This means, that the model predicts the next time slot and uses that prediction as an additional input for the next step in an iterative manner.

Prediction Interval. Since the prediction of time-series data is probabilistic, it is necessary to determine the possible deviation of the forecast. AIROBE needs for each prediction interval the range of the deviation as input in order to optimize the exchange of energy in the system for the next period. We use quantile regression (QR) to elaborate the prediction deviation [50]. QR can be described as follows: $Q_y\left(q \mid X_t\right) = X_t\beta_q$. $Q_y(q|\ *)$ is the conditional q^{t} quantile of the production or consumption distribution (y_t). X_t are the regressors for each quantile, while β_q represents the vector of parameters for the quantile q. Each of the two predictors for the quantiles use the pinball loss function or quantile score (QS), present in (27).

$$\varphi\left(y_t, \hat{y}_{t,q}, q\right) = \begin{cases} \left(1 - \frac{q}{100}\right)\left(\hat{y}_{t,q} - y_t\right) & y_t < \hat{y}_{t,q} \\ \frac{q}{100}\left(y_t - \hat{y}_{t,q}\right) & y_t \geq \hat{y}_{t,q} \end{cases} \tag{27}$$

$\hat{y}_{t,q}$ is the q^{t} quantile of the predicted load and consumption and y_t is the target value for each prediction. The QS is the mean of the pinball losses across all target quantiles [51].

Error Metric. We used the Mean Absolute Percentage Error (MAPE) to evaluate the prediction quality of the machine learning models:

$$MAPE = \frac{1}{n}\sum_{t=1}^{n}\left|\frac{A_t - F_t}{A_t}\right| * 100 \tag{28}$$

where A_t represents the vector of the actual values, F_t the forecasted ones and n is the number of predictions.

5. Evaluation

In this section, we answer the following questions:

1. *Prediction Interval*: How accurate our clustering-based ML-models in predicting the PV power generation and the energy consumption are as well as what the resulting deviation over time for different clusters is?
2. *Robustness*: How do different parameters of AIROBE impact the robustness of the solution, the cost and the state of energy?
3. Price of Robustness: How can AIROBE reduce the Price of Robustness (PoR) and what the impact of the opportunistic model on constraint violation probability is?

5.1. Baselines

We use the following baseline for analysis and comparison with the proposed AIROBE model: as baseline, we use the partial knowledge based model (Section 3.2) which considers uncertainty in both the load and the PV production sides. We call this conventional robust approach which considers the absolute worst-case of PV production and prosumer consumption under a budget of uncertainty. This type of RO based models, was extensively used in the literature as shown in Table 1.

5.2. Experimental setup

The following section illustrates the overall modelling and experimental setups conducted in this work. Fig. 3 presents the workflow of the conducted experiments and modelling and the following subsections explain each part in detail.

5.2.1. Data set

In this study, we validate the effectiveness of the forecasting and scheduling models on the city learn framework data set,[1] representing a single-node MG. The MG contains $n = 9$ residential and non-residential users subscribing in the EMS as shown in Fig. 4. The load represents the heating and the appliances demand. The data set contains the hourly consumption and PV power generation for the different users and the weather information during one year. This step is represented in the first part of Fig. 3, data collection.

5.2.2. PV power generation and energy consumption prediction

The development of the predictors as well as the distribution of the prediction deviation is divided into three main steps: (1.) clustering of the datasets with weather information, (2.) development of the predictors and (3.) estimation of the prediction deviation.

As a first step, we conducted the weather type clustering as described in Section 4 with the available weather features: solar irradiation, temperature and humidity for the whole year of data. With this we retrieved four sub-datasets for each weather condition (sunny, partly overcast, overcast and rainy). Additionally to the weather features, we enrich these datasets with the historical information about the PV power production and energy consumption of the prosumer in the system. The sub-datasets for the four different clusters were divided into a training (80%), validation (10%) and test (10%) dataset. A LightGBM model was trained for the energy consumption and PV power production of each prosumer and weather cluster, individually. The predictor takes 48 h as input to forecast the next 24 h. Additionally, we used grid-search to select the best hyperparameters for each model. To estimate the deviations of the prediction we used the QR and QS as described in Section 4 using 0.90 for the upper boundary and 0.10 for the lower one to build a 80% confidence interval.

5.2.3. Optimization

In our case study, we schedule day-ahead energy exchange where each time slot is equal to 1 hour; with time horizon of $N = 24$ hours, i.e, the decision is made by solving the optimization problem for the

[1] https://github.com/intelligent-environments-lab/CityLearn

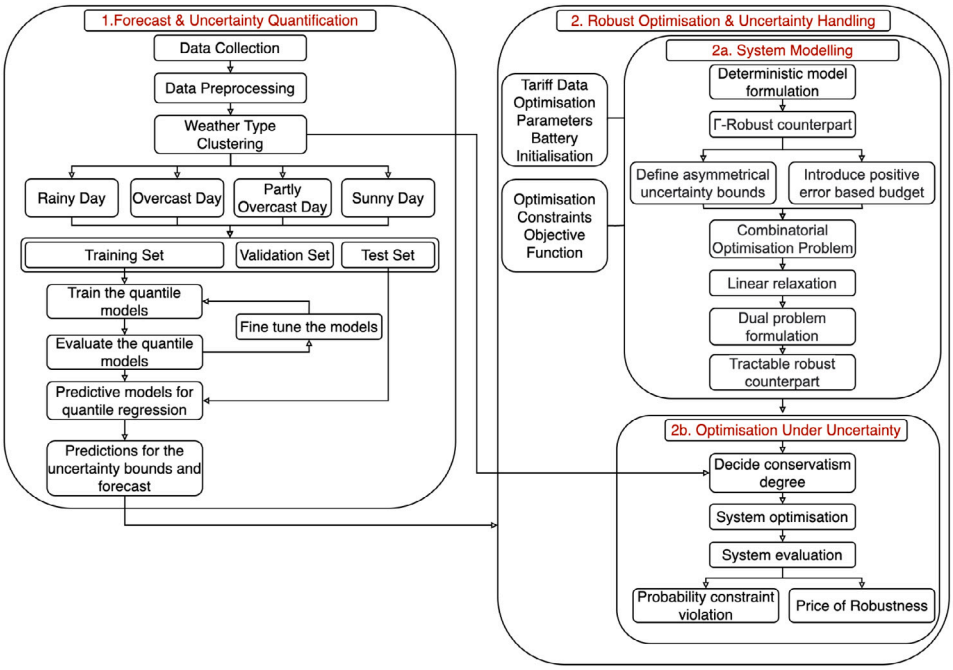

Fig. 3. Flowchart of the modelling and experimental setup.

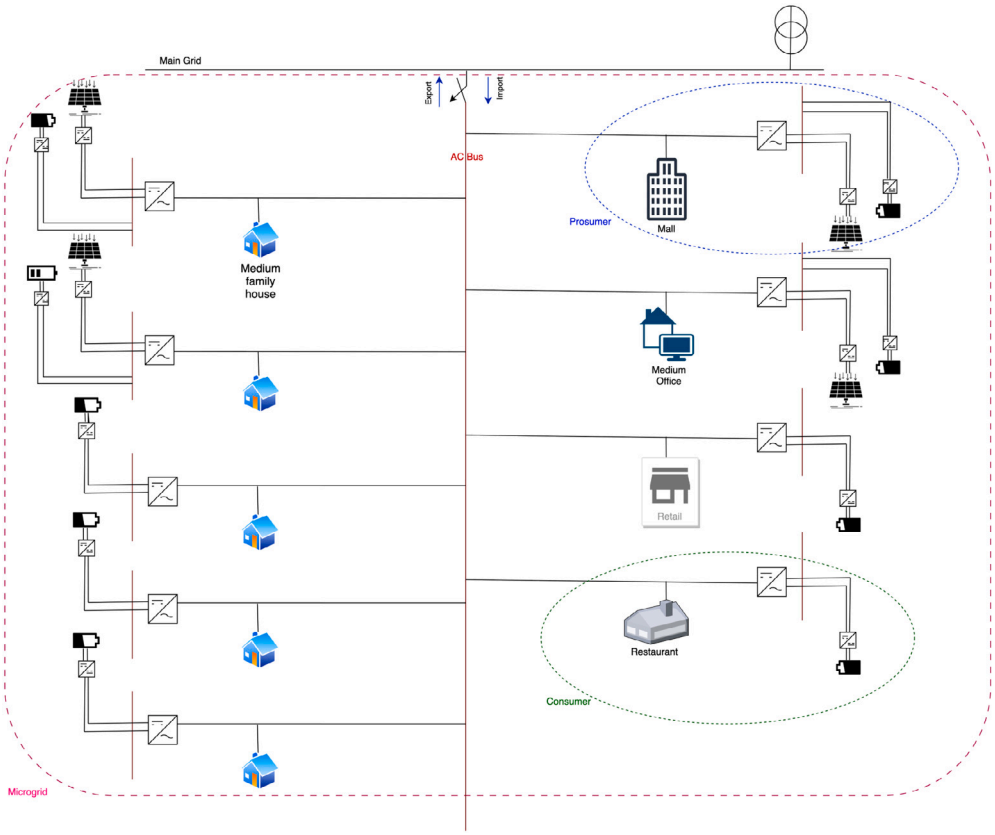

Fig. 4. Microgrid Setup.

Table 2
Production summary for prosumer nine.

Cluster	Average deviation		Overall maximum deviation	Overall minimum deviation	MAPE
	Over prediction	Under prediction			
Rainy	12.97%	21.97%	23.35%	1.15%	5.63%
Partly overcast	15.87%	11.46%	40.31%	1.24%	3.22%
Sunny	30.21%	4.16%	40.42%	1.32%	2.06%
Overcast	54.74%	0.17%	83.09%	0.53%	5.69%

Table 3
Consumption summary for prosumer nine.

Cluster	Average deviation		Overall maximum deviation	Overall minimum deviation	MAPE
	Over prediction	Under prediction			
Rainy	18.72%	16.67%	39.28%	4.03%	6.60%
Partly overcast	17.54%	26.68%	21.28%	4.19%	8.56%
Sunny	9.48%	3.93%	29.91%	1.61%	4.32%
Overcast	30.05%	18.79%	46.55%	3.15%	5.83%

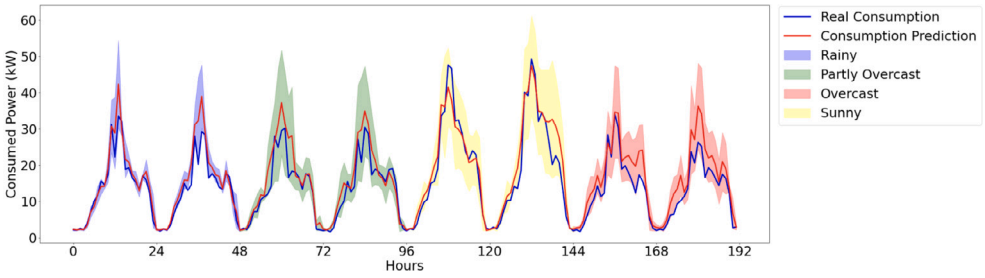

Fig. 5. Consumption prediction and deviation of prosumer nine for each weather cluster.

next $N = 24h$ with a time window from 0: 00 to 23: 59. Hourly import and export prices were obtained from Nord Pool market data.[2] We use the ML predictions for the PV production, the consumption and their deviations as the input to our optimization models, i.e, the reference values. The model is implemented in Python (RSOME library[3]) and solved by Gurobi.[4]

5.3. Prediction quality and uncertainty quantification

Table 2 shows the prediction quality of the produced PV energy for prosumer nine. The table shows the average deviation for the under and over prediction, overall maximum and minimum deviation in percentage and MAPE over the period of 90 days for the weather type clusters. It is visible that the clusters behave differently. For example, the sunny cluster has a stronger deviation towards the over prediction with an average deviation of 30.21% while the average under prediction is 4.16%. This behaviour of good deviations is also visible in the overcast weather cluster. The other weather clusters average deviation for the under and over prediction express a mostly even magnitude towards either bound. In terms of the prediction quality, the sunny cluster has the lowest MAPE of 2.06%. The overcast cluster presents the highest overall maximum deviation of 54.74%. The high maximum deviation occurs when there is a sudden change in the power production. This means, that the day is for example clustered as an overcast day, but the production of the PV panel is higher than predicted due to sudden weather changes (see Figs. 5 and 6).

Table 3 summarizes the prediction quality for the energy consumption. In contrast to the prediction of the PV generation, the MAPE is higher in every weather cluster. However, this is not visible in terms of deviations. The sunny cluster for example, still shows a stronger magnitude in deviation towards the over prediction with 9.48% but it is lower than the 30.21% in Table 2 for the production.

5.4. Robustness

In order to study the impact of the proposed model AIROBE on the objective value, i.e, the MG operational cost, we evaluate the cost under the different types of budget of uncertainty namely: Γ_t^{PV}, Θ_t^{PV}, Γ_t^{PC}, Θ_t^{PC}. We plot the MG aggregated cost in Fig. 7. First, we optimize using the baseline worst-case model under the PV production and consumption uncertainties described in 3.2 and we plot the results in Fig. 7(c). We observe that the cost value increases with the increase of the uncertainty budgets Γ_t^{PV} and Γ_t^{PC}. The values $(\Gamma_t^{PV}, \Gamma_t^{PC}) = (0, 0)$ corresponds to the deterministic baseline described in 3.1 where we do not have any protection. In this deterministic case, we have the lowest cost 2399.89€, however, the future deviations will cause the MG to import on the spot in order to cover the demand which will cause an instability of the MG and yields higher expected cost in the future. The values $(\Gamma_t^{PV}, \Gamma_t^{PC}) = (9, 9)$ correspond to the most-conservative case where we protect from all possible deviation to their lower bounds which yields the highest possible cost 5007.48€. The high cost is explained by the fact that when we protect from the worst case scenario, we expect to produce less, alternatively consume more, which leads the users to import more power and charge their batteries to cover the future demand.

In Fig. 7(a),(b) we optimize using the proposed model AIROBE described in 3.3. In Fig. 7(a) we study the impact of the budgets related to the PV generation uncertainty. We observe that the cost has the

[2] https://www.nordpoolgroup.com
[3] https://xiongpengnus.github.io/rsome/
[4] https://www.gurobi.com

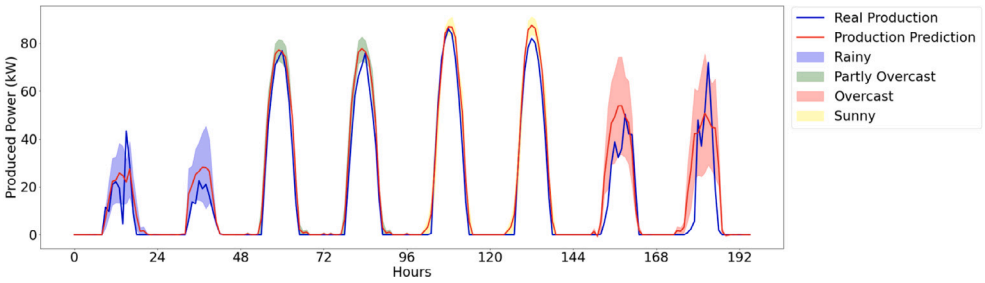

Fig. 6. Production prediction and deviation of prosumer nine for each weather cluster.

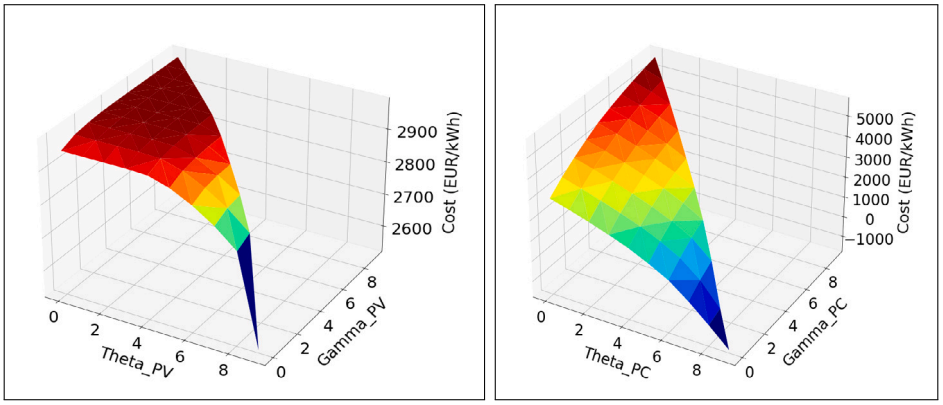

(a) The MG cost distribution under PV uncertainty budgets Γ_t^{PV} and Θ_t^{PV}

(b) The MG cost distribution under load uncertainty budgets Γ_t^{PC} and Θ_t^{PC}

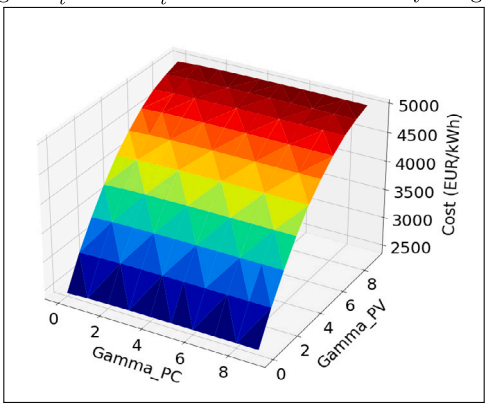

(c) The MG cost distribution under PV uncertainty budgets Γ_t^{PV} and Γ_t^{PC}

Fig. 7. The MG cost distribution under different types of uncertainty.

highest values when $\Theta_t^{PV} = 0$ which represents the same values as in Fig. 7(c) for $\Gamma_t^{PC} = 0$ and corresponds to the baseline value where we do not consider the favourable (positive) deviations. In Fig. 7(a), the cost increases as we increase the budget Γ_t^{PV} for a fixed Θ_t^{PV}. We notice that the cost value decreases as we increase the budget Θ_t^{PV} and hits the minimum value 2527.71€ for $(\Theta_t^{PV}, \Gamma_t^{PV}) = (9, 0)$. In fact, by introducing the budget Θ_t^{PV} which reflects the favourable deviations, the users tend to be more opportunistic and import less compared to the worst-case scenario where they import more than their demand and charge their batteries in order to protect from future worst deviations. However, in a sunny day for example, the PV generated power is likely to deviate to its upper bound as shown in 2. Taking those scenarios into account, makes the scheduling less conservative and reduces the extensive import from the main grid that appears in the worst-case scenario based scheduling.

Similarly, in Fig. 7(b) we plot the aggregated MG cost under the impact of the budgets related to the users consumption uncertainty. The negative values of the cost corresponds to a profit where the MG is expected to make a profit. This scenario might appear when the MG has power generation excess in comparison to the consumption, and the model takes into account these favourable good deviations (the users produce more than expected or consume less than expected). We observe that the two budgets of uncertainty have similar affect on the cost as in Fig. 7(a) where the cost decreases as we increase the budget Θ_t^{PC}. This is explained by the fact that the users consumption might deviate to its lower bound, i.e, the user consume less energy than the predicted value and taking that into account encourages them to import less or charge their batteries less. We can conclude that integrating the favourable deviations into the scheduling, yields lower cost which implies lower power import from the main grid in general.

Fig. 8 presents the aggregated state of the energy (SoE) of seven users, and its variation under different budgets of uncertainty. In Fig. 8(a) we fix $\Theta_t^{PV} = 0$ and optimize for three different budgets of uncertainty related to the PV power generation Γ_t^{PV}. We pick one

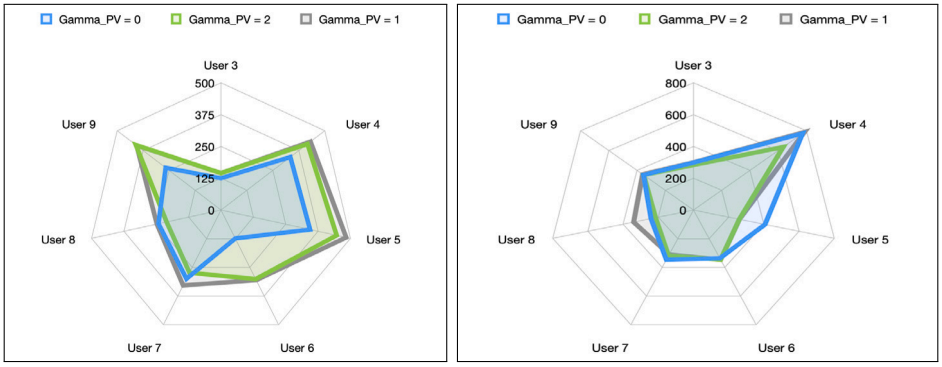

(a) Overall State of Energy of seven users for $\Gamma_t^{PV} = 0, 1, 2$ and $\Theta_t^{PV} = 0$

(b) Overall State of Energy of seven users for $\Gamma_t^{PV} = 0, 1, 2$ and $\Theta_t^{PV} = 2$

Fig. 8. The impact of the different budgets of uncertainty on the overall State of Energy (kWh) of the prosumers batteries.

sunny day in order to showcase the effectiveness of the budget of uncertainty related to the favourable deviations. We observe that the users batteries tend to have a higher SoE when we increase the value of Γ_t^{PV} in Fig. 8(a). In fact, in order to protect from the worst-case scenario, i.e, the bad deviations, the users tend to charge their batteries to replace the expected deficit. In Fig. 8(b) we want to assess the impact of the favourable deviations on the battery behaviour. We fix $\Theta_t^{PV} = 2$, i.e, the model will take into account that two uncertain parameters will deviate to their upper bound. We observe that the SoE has increased in general. This is due to the fact that higher expected generated PV power were taken into account in the optimization scheduling and the users charge their batteries with that excess or provide it to the MG utilization which means other users with deficit will tend to charge their batteries as well.

5.5. Price of robustness

To show the impact of data uncertainty on the objective value, i.e, the MG operational cost, and to demonstrate the effectiveness of the proposed approach against it, we simulate 10 000 scenarios of random yields for users production and then we compare the robust solutions generated by varying the level of the uncertainty budgets Γ_t^{PV} and Θ_t^{PV}. For simplification and without loss of generality, we fix Γ^{PC} and Θ_t^{PC} to zero. We evaluate the constraint violation probability and the Price of Robustness. We define the PoR rate as the relative difference between the costs realized by the robust solution and the nominal solution where we do not protect against the uncertainty. The PoR is used to quantify the extra MG cost required to cover for the robust solution. We calculate the PoR as follow:

$$PoR = 100\frac{|Cost_{\Gamma=0} - Cost_{\Gamma>0}|}{|Cost_{\Gamma=0}|} \tag{29}$$

Fig. 9(a) shows the PoR rate variation as we increase the worst-case scenario budget of uncertainty Γ_t^{PV} for different fixed values of Θ_t^{PV}. The case where $\Theta_t^{PV} = 0$, which corresponds to the baseline model, yields the highest value of PoR, alternatively the highest cost. The value of PoR increases as we increase the budget Γ_t^{PV} since we are protecting more against the worst-case scenario, where the higher Γ_t^{PV} the more uncertain variables deviate to their lower bound corresponding to less PV power production. In Fig. 9(a) we compute the PoR for different values of Θ_t^{PV} which indicates that some uncertain variables will deviate to their upper bound, i.e, the PVs will generate more power than expected, which mostly corresponds to sunny days. The PoR is reduced as we introduce the good deviations in our scheduling. The objective value is reduced by 0.82% atmost for $\Theta_t^{PV} = 4$ compared to 1.92% PoR for the classical worst-case model, i.e, $\Theta_t^{PV} = 0$. Fig. 9(b) illustrates the probability of constraint violation for different levels of protection Γ_t^{PV}. The probability of constraint violation decreases when

Table 4
Summary of the results under different types of protection.

$(\Gamma_t^{PV}, \Theta_t^{PV}, \Gamma_t^{PC}, \Theta_t^{PC})$	Cost (€)	PoR (%)	Constraint Violation Prob
(0, 0, 0, 0)	2399.89	0	1
(9, 0, 9, 0)	5007.48	–	–
(0, 9, 0, 0)	2527.71	–	1
(0, 0, 0, 9)	−1623.33	–	–
(9, 0, 0, 0)	4607.78	1.92	0
(6, 0, 0, 0)	4511.79	1.88	0.04
(6, 1, 0, 0)	3839.82	1.6	0.04
(6, 3, 0, 0)	3071.5	1.28	0.04
(4, 0, 0, 0)	3863.82	1.61	0.56
(4, 1, 0, 0)	3095.85	1.29	0.56
(4, 3, 0, 0)	2927.86	1.22	0.56
(2, 0, 0, 0)	2423.88	1.01	0.91

Table 5
Solving time summary.

Solving time (s)	Min	Max	Average
	0.2344	27.438	5.982

we increase the level of protection until it reaches the value 0. This is explained by the fact that the more we protect against the uncertainty, the more probable it is that we achieve energy balance and meet our demand. We note that we compute the probability of constraint violation for the different values of Θ_t^{PV}, which remains unchangeable. We conclude that the proposed model reduces the PoR and exhibit lower MG costs while conserving the same level of protection. We summarize some of the findings in Table 4 for different values of the uncertainty budgets. We showcase the extreme situations such as zero protection, or conservative solution. The missing values in Table 4 are due the fact that we only assume uncertainty in the production when assessing the PoR and the constraint violation probability. Table 5 presents a summary of the computational time spent we the solving process. For a fixed value of the quadruple of $(\Gamma_t^{PV}, \Theta_t^{PV}, \Gamma_t^{PC}, \Theta^{PC})$, the solver needs between 0.2344 and 27.438 s to solve the optimization problem. Due to space constraints, we only include a summary of the solving time (min, max, average).

5.6. Case study of a rainy day

In this section, we investigate the robustness of the proposed solution in difficult weather situations, such as rainy days. We choose one day from the rainy cluster where the negative deviation is significant. Table 6 shows the uncertainty quantification of prosumer four,i.e, the lower bound predicted percentage (negative deviation), and the production forecast. We also include the actual production and the actual deviation of the forecast from the actual production. We can

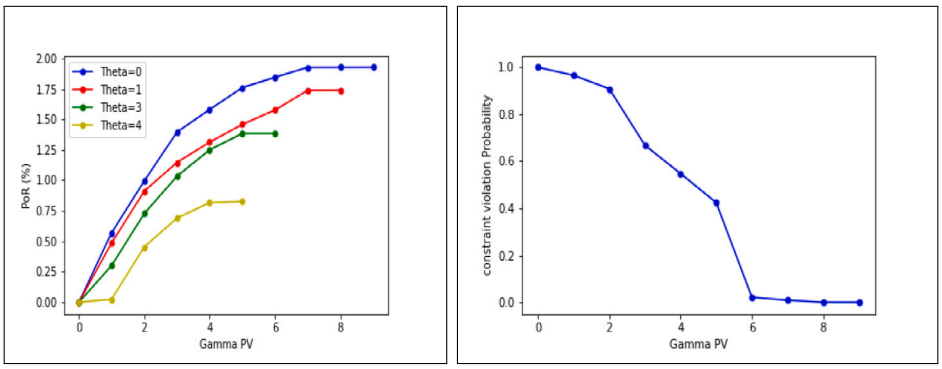

(a) Price of Robustness rate for different values of good deviation budgets Θ_t^{PV} (b) Probability of Constraint Violation for different values of Θ_t^{PV}

Fig. 9. Evaluation of the AIROBE robustness performance in terms of the good and bad deviations.

Table 6
Example of Uncertainty Quantification for prosumer four during a rainy day.

Time (h)	1	2	3	4	5	6	7	8	9	10	11	12	13	14	15	16	17	18	19	20	21	22	23	24
Production (kW)	0	0	0	0	0	0	0	0.77	2.63	4.01	4.7	4.26	4.4	3.73	2.64	1.31	0	0	0	0	0	0	0	0
Prediction (kW)	0	0	0	0	0	0	0	1.12	3.19	5.02	5.85	6	5.73	5.47	2.99	1.95	0	0	0	0	0	0	0	0
Lower_bound(%)	0	0	0	0	0	0	0	−50	−47.65	−61.16	−65.98	−61.5	−60.03	−59.41	−51.51	−69.23	0	0	0	0	0	0	0	0
Actual_deviation (%)	0	0	0	0	0	0	0	−45.45	−21.29	−25.18	−24.46	−40.84	−30.22	−46.64	−13.25	−48.85	0	0	0	0	0	0	0	0

Table 7
Supply–demand balance assessment for rainy day: comparison between AIROBE and uncertainty fixed range 10%, under worse case scenarios.

MG energy transactions (kW)	Actual supply	Actual demand	Actual balance	Unplanned Imp (10%)	Unplanned Imp (AIROBE)
	347.08	2671	(-) 2480.35	(-) 308.83	(-) 77.05
Operational cost (€)	–	–	–	70.41	17.56

notice that the prediction is higher than the actual production, which means the forcasting model is over-predicting the PV energy. The lower bound of the uncertainty is significant. In these situations, it is extremely important to protect against the bad deviations. In order to investigate the protection performance of the proposed model, we optimize the MG operations during the rainy day from Table 6, under the worse case scenario. First, we optimize using the predicted uncertainty ranges. Then, we optimize using a worse case scenario model with fixed symmetrical uncertainty range equal to 10% for all time slots [18,23,25]. We simplify the analysis by considering uncertainty only uncertain production, while assuming that consumption values remain fixed and known. Table 7 shows the balance and corresponding cost for each model. The actual supply and demand correspond to the true measured values from the city learn data. The actual balance −2480.35 kW, is the difference between the total supply and demand, which is in this situation negative and corresponds to the total deficit of the MG during the day, and needs to be covered. After optimization under the worse case scenario, the model with fixed uncertainty yields an unplanned import equal to 308.83 kW while our model that uses the predicted uncertainty yields lower unplanned import equal to 77.05 kW. Capturing the negative deviation instead of fixed range is more realistic and help reduce the unplanned energy transactions with the main grid, under rainy days. We use the import prices to calculate the cost of the unplanned import in Table 7, however, it is important to note that some systems would charge penalties in these situations which will increase the cost.

6. Discussion

6.1. Budgets of uncertainty

In the proposed formulation, the MG optimal scheduling schemes can be made robust by adjusting the two types of uncertainty budgets Γ_t and Θ_t. The decision-maker faces a trade-off between protecting the constraint (demand–supply balance) and the degree of solution conservatism. The uncertainty budgets, Γ_t and Θ_t, are input to the robust formulation and allow the decision-maker to adjust it based on their risk aversion. A larger Γ_t implies a more conservative approach which can be beneficial in extreme weather situation, emergencies or high prices where the decision maker strategy is to be conservative rather than opportunistic. However, protecting against the absolute worst-case is not always beneficial for the system, and may yield in unplanned surplus. The decision maker, in these situations, can decide to include positive deviations (Θ_t) in the system. Consequently, decision-makers or operators can choose an appropriate Γ_t and Θ_t in two ways: (1) using a probabilistic bound for constraint violation or (2) exhaustively testing different Γ_t and Θ_t values to find the best fit for their specific interests. While the second approach is more attractive in balancing the budgets with other decisions, it may not be recommended for problems that require significantly long solving times.

6.2. Limitations and next steps

AIROBE took an initial step in formulating a robust MGs energy scheduling model, that accounts for time-varying prediction uncertainties. Unlike classical Γ-robustness models and previous work, we consider asymmetric uncertainty ranges under bad and good deviations, which allows us to calculate more opportunistic solutions. In this section, we describe limitations of the current model and possible future directions. AIROBE assumes that the battery capacity is constant and neglects the degradation of the battery life over time because we evaluate our scheduling over a short period of time. In real life, the battery is impacted by the charging and discharging cycles and degrades over time which can impact both the cost and the solver decisions. Adding such battery constraints, a battery-related cost to the objective

function and evaluating over a long period of time is a possible next step in this work. While our current model assumes that the different uncertain parameters are independent, the PV power generation and less so the load profiles maybe subject to geographical and temporal correlation. AIROBE can be extended to consider the correlation of the uncertain parameters and study its impact on the robustness and the budget of uncertainty, in a multi-microgrids settings. Additionally, while the proposed solution accounts for the overall benefit of the community, in a cooperation manner, and helps the decision makers to make better decisions for the microgrid under uncertainties, the customers could have incentives to engage in arbitrage. Arbitrage is the practice of exploiting price differences in different markets to gain profits. In this context, households might adjust their energy consumption patterns based on the prices they observe, taking advantage of low prices and reducing consumption during high-price periods. Finally, an area of further research is to extend AIROBE for other DERs such as wind power and consider the curtailment cost.

7. Conclusion

In this paper we presented AIROBE, a MGs energy management robust optimization model that schedules the MGs operations under PV power generation and consumption uncertainties, in an effective and opportunistic manner. We use time-series prediction technique using clustering in order to forecast PV power generation and energy demand that are needed for the model input. We discussed the limitations of the classical worst-case robust optimization based approach and motivated the need to integrate more accurate uncertainty ranges, i,e, asymmetric and time-varying deviation ranges. We proposed a less conservative robust approach that accounts for the good deviations in a MG and demonstrated that AIROBE reduces the Price of Robustness while maintaining the same level of protection.

Declaration of competing interest

The authors declare the following financial interests/personal relationships which may be considered as potential competing interests: Andreas Kassler reports financial support was provided by Energimyndigheten of Sweden. Andreas Kassler reports a relationship with Energimyndigheten of Sweden that includes: funding grants.

Data availability

Data will be made available on request.

Acknowledgements

This work has been partly funded by the Energy Agency of Sweden (Energimyndigheten) through the AI4-ENERGI project (Projektnr: 50246-1) and the project Solar Electricity Research Centre, Sweden (SOLVE), grant number 52693-1. Additional funding has been provided by the Bavarian State Ministry for Science and Art through the Hightech Agenda (HTA).

Appendix. Proofs

We provide here the proof of Proposition 1.

Proposition. For each time period $t \in T$, the robust counterpart of constraint (9) when protection for Γ_t^{PV} "bad" deviations and Θ_t^{PV} "good" deviations of PV generation coefficients and Γ_t^{PC} "bad" deviations and Θ_t^{PC} "good" deviations of load coefficients are allowed in period t writes as:

$$\sum_{j\in C}\left[\bar{p}_{j,t}^{PV}+\left(b_{j,t}^{dis}-b_{j,t}^{ch}\right)\right]-\left(\Gamma_t^{PV}\cdot v_t^{PV-}-\Theta_t^{PV}\cdot v_t^{PV+}+\sum_{j\in C}w_{j,t}^{PV}\right)+\left(p_t^{imp}-p_t^{exp}\right)\geq\sum_{j\in C}\bar{p}_{j,t}^{PC}+\left(\Gamma_t^{PC}\cdot v_t^{PC+}-\Theta_t^{PC}\cdot v_t^{PC-}+\sum_{j\in C}w_{j,t}^{PC}\right) \quad \text{(A.1)}$$

$$v_t^{PV-}+w_{j,t}^{PV}\geq\delta_{j,t}^{PV-} \qquad \forall j\in C \qquad \text{(A.2)}$$

$$-v_t^{PV+}+w_{j,t}^{PV}\geq-\delta_{j,t}^{PV+} \qquad \forall j\in C \qquad \text{(A.3)}$$

$$v_t^{PC+}+w_{j,t}^{PC}\geq\delta_{j,t}^{PC+} \qquad \forall j\in C \qquad \text{(A.4)}$$

$$-v_t^{PC-}+w_{j,t}^{PC}\geq-\delta_{j,t}^{PC-} \qquad \forall j\in C \qquad \text{(A.5)}$$

$$v_t^{PV+},\ v_t^{PV-}\geq 0 \qquad \text{(A.6)}$$

$$w_{j,t}^{PV}\geq 0 \qquad \forall j\in C \qquad \text{(A.7)}$$

$$v_t^{PC+},\ v_t^{PC-}\geq 0 \qquad \text{(A.8)}$$

$$w_{j,t}^{PC}\geq 0 \qquad \forall j\in C \qquad \text{(A.9)}$$

Proof. In order to prove this result, we first focus attention on a time period $t \in T$ and define a robust version of the constraint load satisfaction constraint (9) in which we include terms:

- $-DEV(\Gamma_t^{PV},\Theta_t^{PV})$ to represent the worst decrease that the left-hand-side of the constraint may experience for Γ_t^{PV} bad deviations and Θ_t^{PV} good deviations of the PV coefficients;
- $+DEV(\Gamma_t^{PC},\Theta_t^{PC})$ to represent the worst increase that the right-hand-side of the constraint may experience for Γ_t^{PC} bad deviations and Θ_t^{PC} good deviations of the load coefficients.

This constraint writes as:

$$\sum_{j\in C}\left[\bar{p}_{j,t}^{PV}+\left(b_{j,t}^{dis}-b_{j,t}^{ch}\right)\right]-DEV(\Gamma_t^{PV},\Theta_t^{PV})+\left(p_t^{imp}-p_t^{exp}\right)\geq\sum_{j\in C}\bar{p}_{j,t}^{PC} \quad \text{(A.10)}$$

The value $DEV(\Gamma_t^{PV},\Theta_t^{PV})$ corresponds to the optimal value of the following combinatorial optimization problem:

$$DEV(\Theta_t^{PV},\Gamma_t^{PV})=\max\sum_{j\in C}\left(\delta_{j,t}^{PV-}\cdot z_{j,t}^{-}-\delta_{j,t}^{PV+}\cdot z_{j,t}^{+}\right) \quad \text{(A.11)}$$

$$\sum_{j\in C}z_{j,t}^{PV-}\leq\Gamma_t^{PV} \quad \text{(A.12)}$$

$$\sum_{j\in C}z_{j,t}^{PV+}\geq\Theta_t^{PV} \quad \text{(A.13)}$$

$$z_{j,t}^{PV-}+z_{j,t}^{PV+}\leq 1 \qquad \forall j\in C \quad \text{(A.14)}$$

$$z_{j,t}^{PV-}\in\{0,1\} \qquad \forall j\in C \quad \text{(A.15)}$$

$$z_{j,t}^{PV+}\in\{0,1\} \qquad \forall j\in C \quad \text{(A.16)}$$

in which:

- a binary variable $z_{j,t}^{PV-}$ (A.15) is equal to 1 if coefficient $\bar{p}_{j,t}^{PV}$ experiences the largest bad deviation (decrease of PV generation) $\delta_{j,t}^{PV-}$ and to 0 otherwise;
- a binary variable $z_{j,t}^{PV+}$ (A.16) is equal to 1 if coefficient $\bar{p}_{j,t}^{PV}$ experiences the largest good deviation (increase of PV generation) $\delta_{j,t}^{PV+}$ and to 0 otherwise;
- the constraint (A.12) imposes that at most Γ_t^{PV} bad deviations may occur;
- the constraint (A.13) imposes that at least Θ_t^{PV} good deviations must occur;
- the constraints (A.14) impose that each coefficient may experience at most one kind of deviation (either bad or good);
- the objective function (A.11) pursues the maximization of the worst reduction in value of the left-hand-side of constraint due to the summation of bad and good deviations;

Let us now consider the linear relaxation of the previous combinatorial optimization problem, i.e. the following problem in which the integrality requirement (A.15), (A.16) on the binary variables is removed and

they can assume any value between 0 and 1:

$$DEV(\Theta_t^{PV}, \Gamma_t^{PV}) = \max \sum_{j\in C} \left(\delta_{j,t}^{PV-} \cdot z_{j,t}^{-} - \delta_{j,t}^{PV+} \cdot z_{j,t}^{+}\right) \quad \text{(A.17)}$$

$$\sum_{j\in C} z_{j,t}^{PV-} \le \Gamma_t^{PV} \quad \text{(A.18)}$$

$$\sum_{j\in C} z_{j,t}^{PV+} \ge \Theta_t^{PV} \quad \text{(A.19)}$$

$$z_{j,t}^{PV-} + z_{j,t}^{PV+} \le 1 \qquad \forall j \in C \quad \text{(A.20)}$$

$$0 \le z_{j,t}^{PV-} \le 1 \qquad \forall j \in C \quad \text{(A.21)}$$

$$0 \le z_{j,t}^{PV+} \le 1 \qquad \forall j \in C \quad \text{(A.22)}$$

It can be noted that its bínary coefficient matrix is totally unimodular [42]. Consequently, the optimal solution of the linear relaxation problem is integral and provides an optimal solution also for the combinatorial optimization problem.

We can then define the dual problem of the linear relaxation:

$$DEV(\Theta_t^{PV}, \Gamma_t^{PV}) = \min \ \Gamma_t^{PV} \cdot v_t^{PV-} - \Theta_t^{PV} \cdot v_t^{PV+} + \sum_{j\in C} w_{j,t}^{PV} \quad \text{(A.23)}$$

$$v_t^{PV-} + w_{j,t}^{PV} \ge \delta_{j,t}^{PV-} \qquad \forall j \in C \quad \text{(A.24)}$$

$$-v_t^{PV+} + w_{j,t}^{PV} \ge -\delta_{j,t}^{PV+} \qquad \forall j \in C \quad \text{(A.25)}$$

$$v_t^{PV+},\ v_t^{PV-} \ge 0 \quad \text{(A.26)}$$

$$w_{j,t}^{PV} \ge 0 \qquad \forall j \in C \quad \text{(A.27)}$$

By duality theory, since the linear relaxation (A.17)–(A.22) is finite and optimal, also its dual problem (A.23)–(A.27) is finite and optimal and the optimal values of the two problems coincide. Consequently, we can use the dual problem to substitute the term $DEV(\Gamma_t^{PV}, \Theta_t^{PV})$ in the robust constraint (A.10), as specified in [42].

We can proceed in the same way for dealing with the deviation term $+DEV(\Gamma_t^{PC}, \Theta_t^{PC})$ appearing in the right-hand-side of the constraint (9). Specifically, the value $DEV(\Gamma_t^{PC}, \Theta_t^{PC})$ corresponds to the optimal value of the following combinatorial optimization problem:

$$DEV(\Theta_t^{PC}, \Gamma_t^{PC}) = \max \sum_{j\in C} \left(\delta_{j,t}^{PC+} \cdot z_{j,t}^{+} - \delta_{j,t}^{PC-} \cdot z_{j,t}^{-}\right) \quad \text{(A.28)}$$

$$\sum_{j\in C} z_{j,t}^{PC+} \le \Gamma_t^{PC} \quad \text{(A.29)}$$

$$\sum_{j\in C} z_{j,t}^{PC-} \ge \Theta_t^{PC} \quad \text{(A.30)}$$

$$z_{j,t}^{PC-} + z_{j,t}^{PC+} \le 1 \qquad \forall j \in C \quad \text{(A.31)}$$

$$z_{j,t}^{PC-} \in \{0,1\} \qquad \forall j \in C \quad \text{(A.32)}$$

$$z_{j,t}^{PC+} \in \{0,1\} \qquad \forall j \in C \quad \text{(A.33)}$$

in which:

- a binary variable $z_{j,t}^{PC-}$ (A.32) is equal to 1 if coefficient $\bar{p}_{j,t}^{PC}$ experiences the largest good deviation (decrease of load) $\delta_{j,t}^{PC-}$ and to 0 otherwise;
- a binary variable $z_{j,t}^{PC+}$ (A.33) is equal to 1 if coefficient $\bar{p}_{j,t}^{PC}$ experiences the largest bad deviation (increase of load) $\delta_{j,t}^{PV+}$ and to 0 otherwise;
- the constraint (A.29) imposes that at most Γ_t^{PC} bad deviations may occur;
- the constraint (A.30) imposes that at least Θ_t^{PC} good deviations must occur;
- the constraints (A.31) impose that each coefficient may experience at most one kind of deviation (either bad or good);
- the objective function (A.28) pursues the maximization of the worst increase in value of the right-hand-side of constraint due to the summation of bad and good deviations;

Also for the previous combinatorial optimization problem, we can define its linear relaxation, removing the integrality requirement on the binary variables:

$$DEV(\Theta_t^{PC}, \Gamma_t^{PC}) = \max \sum_{j\in C} \left(\delta_{j,t}^{PV+} \cdot z_{j,t}^{+} - \delta_{j,t}^{PV-} \cdot z_{j,t}^{-}\right) \quad \text{(A.34)}$$

$$\sum_{j\in C} z_{j,t}^{PV+} \le \Gamma_t^{PC} \quad \text{(A.35)}$$

$$\sum_{j\in C} z_{j,t}^{PC-} \ge \Theta_t^{PC} \quad \text{(A.36)}$$

$$z_{j,t}^{PC-} + z_{j,t}^{PC+} \le 1 \qquad \forall j \in C \quad \text{(A.37)}$$

$$0 \le z_{j,t}^{PC-} \le 1 \qquad \forall j \in C \quad \text{(A.38)}$$

$$0 \le z_{j,t}^{PC+} \le 1 \qquad \forall j \in C \quad \text{(A.39)}$$

In this case, the binary coefficient matrix is also totally unimodular [42] and thus the optimal solution of the linear relaxation problem is integral and provides an optimal solution also for the combinatorial optimization problem.

Therefore, we can define the dual problem of the linear relaxation:

$$DEV(\Theta_t^{PC}, \Gamma_t^{PC}) = \min \ \Gamma_t^{PC} \cdot v_t^{PC+} - \Theta_t^{PC} \cdot v_t^{PC-} + \sum_{j\in C} w_{j,t}^{PC} \quad \text{(A.40)}$$

$$v_t^{PC+} + w_{j,t}^{PC} \ge \delta_{j,t}^{PC+} \qquad \forall j \in C \quad \text{(A.41)}$$

$$-v_t^{PC-} + w_{j,t}^{PC} \ge -\delta_{j,t}^{PC-} \qquad \forall j \in C \quad \text{(A.42)}$$

$$v_t^{PC+},\ v_t^{PC-} \ge 0 \quad \text{(A.43)}$$

$$w_{j,t}^{PC} \ge 0 \qquad \forall j \in C \quad \text{(A.44)}$$

Finally, we can use the dual problems (A.23)–(A.27) and (A.40)–(A.44) to substitute the terms $DEV(\Gamma_t^{PV}, \Theta_t^{PV})$ and $DEV(\Gamma_t^{PC}, \Theta_t^{PC})$ in, thus obtaining the robust optimization model (A.1)–(A.9) and completing the proof. □

References

[1] R.H. Lasseter, P. Paigi, Microgrid: a conceptual solution, in: 2004 IEEE 35th Annual Power Electronics Specialists Conference (IEEE Cat. No.04CH37551), vol. 6, 2004, pp. 4285–4290 Vol.6.

[2] N. Hatziargyriou, H. Asano, R. Iravani, C. Marnay, Microgrids, IEEE Power Energy Mag. 5 (4) (2007) 78–94.

[3] T.S. Ustun, C. Ozansoy, A. Zayegh, Recent developments in microgrids and example cases around the world—A review, Renew. Sustain. Energy Rev. 15 (8) (2011) 4030–4041.

[4] Z. Liu, Q. Wu, S. Huang, H. Zhao, Transactive energy: A review of state of the art and implementation, in: 2017 IEEE Manchester PowerTech, 2017, pp. 1–6.

[5] C. Chen, S. Duan, T. Cai, B. Liu, G. Hu, Smart energy management system for optimal microgrid economic operation, Vol. 5, No. 3, Wiley and the Institution of Engineering and Technology, 2011, pp. 258–267.

[6] F. Farzan, S. Lahiri, M. Kleinberg, K. Gharieh, M. Jafari, Microgrids for fun and profit: The economics of installation investments and operations, Power Energy Mag. IEEE 11 (2013) 52–58.

[7] A. Agüera-Pérez, J.C. Palomares-Salas, J.J. González de la Rosa, O. Florencias-Oliveros, Weather forecasts for microgrid energy management: Review, discussion and recommendations, Appl. Energy 228 (2018) 265–278.

[8] P. Samadi, H. Mohsenian-Rad, V.W.S. Wong, R. Schober, Tackling the load uncertainty challenges for energy consumption scheduling in smart grid, IEEE Trans. Smart Grid 4 (2) (2013) 1007–1016.

[9] K.P. Kumar, B. Saravanan, Recent techniques to model uncertainties in power generation from renewable energy sources and loads in microgrids – A review, Renew. Sustain. Energy Rev. 71 (2017) 348–358, http://dx.doi.org/10.1016/j.rser.2016.12.063.

[10] A. Baziar, A. Kavousi-Fard, Considering uncertainty in the optimal energy management of renewable micro-grids including storage devices, Renew. Energy 59 (2013) 158–166, http://dx.doi.org/10.1016/j.renene.2013.03.026.

[11] S. Sukumar, H. Mokhlis, S. Mekhilef, K. Naidu, M. Karimi, Mix-mode energy management strategy and battery sizing for economic operation of grid-tied microgrid, Energy 118 (2017) 1322–1333, http://dx.doi.org/10.1016/j.energy.2016.11.018.

[12] M.H. Amrollahi, S.M.T. Bathaee, Techno-economic optimization of hybrid photovoltaic/wind generation together with energy storage system in a stand-alone micro-grid subjected to demand response, Appl. Energy 202 (2017) 66–77, http://dx.doi.org/10.1016/j.apenergy.2017.05.116.
[13] C. Chen, S. Duan, T. Cai, B. Liu, G. Hu, Smart energy management system for optimal microgrid economic operation, Renew. Power Gener. IET 5 (2011) 258–267, http://dx.doi.org/10.1049/iet-rpg.2010.0052.
[14] S. Chakraborty, M. Weiss, M. Simoes, Distributed intelligent energy management system for a single-phase high-frequency AC microgrid, Ind. Electron. IEEE Trans. 54 (2007) 97–109, http://dx.doi.org/10.1109/TIE.2006.888766.
[15] T. Niknam, A. Kavousifard, S. Tabatabaei, J. Aghaei, Optimal operation management of fuel cell/wind/photovoltaic power sources connected to distribution networks, Lancet 196 (2011) http://dx.doi.org/10.1016/j.jpowsour.2011.05.081.
[16] T. Niknam, H. Zeinoddini-Meymand, H. Doagou, An efficient algorithm for multi-objective optimal operation management of distribution network considering fuel cell power plants, Energy 36 (2011) 119–132, http://dx.doi.org/10.1016/j.energy.2010.10.062.
[17] A. Mehrizi-Sani, A.H. Etemadi, C.A. Cañizares, R. Iravani, M. Kazerani, A.H. Hajimiragha, O. Gomis-Bellmunt, M. Saeedifard, R. Palma-Behnke, G. Jiménez-Estévez, N.D. Hatziargyriou, Trends in microgrid control IEEE-PES task force on microgrid control, 2014.
[18] E. Kuznetsova, Y.-F. Li, C. Ruiz, E. Zio, An integrated framework of agent-based modelling and robust optimization for microgrid energy management, Appl. Energy 129 (2014) 70–88, http://dx.doi.org/10.1016/j.apenergy.2014.04.024.
[19] Y. Xiang, J. Liu, Y. Liu, Robust energy management of microgrid with uncertain renewable generation and load, IEEE Trans. Smart Grid 7 (2015) 1, http://dx.doi.org/10.1109/TSG.2014.2385801.
[20] W. Hu, P. Wang, H. Gooi, Toward optimal energy management of microgrids via robust two-stage optimization, IEEE Trans. Smart Grid PP (2016) 1, http://dx.doi.org/10.1109/TSG.2016.2580575.
[21] Z. LUO, W. Gu, Z. Wu, Z. Wang, Y. Tang, A robust optimization method for energy management of CCHP microgrid, J. Mod. Power Syst. Clean Energy 6 (2017) http://dx.doi.org/10.1007/s40565-017-0290-3.
[22] L. Wang, Q. Li, R. Ding, M. Sun, G. Wang, Integrated scheduling of energy supply and demand in microgrids under uncertainty: A robust multi-objective optimization approach, Energy 130 (2017) 1–14.
[23] C. Zhang, Y. Xu, Z.Y. Dong, J. Ma, Robust operation of microgrids via two-stage coordinated energy storage and direct load control, IEEE Trans. Power Syst. 32 (4) (2017) 2858–2868.
[24] A. Hussain, V.-H. Bui, H.-M. Kim, Robust optimal operation of AC/DC hybrid microgrids under market price uncertainties, IEEE Access 6 (2018) 2654–2667.
[25] S.M. Hosseini, R. Carli, M. Dotoli, Robust optimal energy management of a residential microgrid under uncertainties on demand and renewable power generation, IEEE Trans. Autom. Sci. Eng. 18 (2) (2021) 618–637, http://dx.doi.org/10.1109/TASE.2020.2986269.
[26] A. Baziar, A. Kavousi-Fard, Considering uncertainty in the optimal energy management of renewable micro-grids including storage devices, Renew. Energy 59 (2013) 158–166, http://dx.doi.org/10.1016/j.renene.2013.03.026.
[27] A. Zakariazadeh, S. Jadid, P. Siano, Smart microgrid energy and reserve scheduling with demand response using stochastic optimization, Int. J. Electr. Power Energy Syst. 63 (2014) 523–533, http://dx.doi.org/10.1016/j.ijepes.2014.06.037.
[28] M.-C. Hu, S.-Y. Lu, Y.-H. Chen, Stochastic programming and market equilibrium analysis of microgrids energy management systems, Energy 113 (2016) 662–670, http://dx.doi.org/10.1016/j.energy.2016.07.061.
[29] P. Kou, D. Liang, L. Gao, Stochastic energy scheduling in microgrids considering the uncertainties in both supply and demand, IEEE Syst. J. 12 (3) (2018) 2589–2600.
[30] X. Wu, X. Hu, X. Yin, S.J. Moura, Stochastic optimal energy management of smart home with PEV energy storage, IEEE Trans. Smart Grid 9 (3) (2018) 2065–2075.
[31] S. Golshannavaz, S. Afsharnia, P. Siano, A comprehensive stochastic energy management system in reconfigurable microgrids: A comprehensive stochastic energy management system, Int. J. Energy Res. 40 (2016) http://dx.doi.org/10.1002/er.3536.
[32] G. Liu, M. Starke, B. Xiao, X. Zhang, K. Tomsovic, Microgrid optimal scheduling with chance-constrained islanding capability, Electr. Power Syst. Res. 145 (2017) 197–206, http://dx.doi.org/10.1016/j.epsr.2017.01.014.
[33] J. Liu, H. Chen, W. Zhang, B.J. Yurkovich, G. Rizzoni, Energy management problems under uncertainties for grid-connected microgrids: A chance constrained programming approach, IEEE Trans. Smart Grid 8 (2017) 2585–2596.
[34] S.A. Alavi, A. Ahmadian, M. Aliakbar-Golkar, Optimal probabilistic energy management in a typical micro-grid based-on robust optimization and point estimate method, Energy Convers. Manage. 95 (2015) 314–325, http://dx.doi.org/10.1016/j.enconman.2015.02.042.
[35] C. Guo, X. Wang, Y. Zheng, F. Zhang, Real-time optimal energy management of microgrid with uncertainties based on deep reinforcement learning, Energy 238 (2022) 121873, http://dx.doi.org/10.1016/j.energy.2021.121873.
[36] J. Yang, M. Yang, M. Wang, P. Du, Y. Yu, A deep reinforcement learning method for managing wind farm uncertainties through energy storage system control and external reserve purchasing, Int. J. Electr. Power Energy Syst. 119 (2020) 105928, http://dx.doi.org/10.1016/j.ijepes.2020.105928.
[37] T. Yang, L. Zhao, W. Li, A.Y. Zomaya, Dynamic energy dispatch strategy for integrated energy system based on improved deep reinforcement learning, Energy 235 (2021) 121377, http://dx.doi.org/10.1016/j.energy.2021.121377.
[38] Y. Wang, D. Qiu, F. Teng, G. Strbac, Towards microgrid resilience enhancement via mobile power sources and repair crews: A multi-agent reinforcement learning approach, IEEE Trans. Power Syst. (2023) 1–17, http://dx.doi.org/10.1109/TPWRS.2023.3240479.
[39] D. Bertsimas, M. Sim, The price of robustness, Oper. Res. 52 (1) (2004) 35–53.
[40] Z. Foroozandeh, I. Tavares, J. Soares, S. Ramos, Z. Vale, Robust energy scheduling for smart buildings considering uncertainty in PV generation, in: 2022 9th International Conference on Electrical and Electronics Engineering, ICEEE, 2022, pp. 245–249, http://dx.doi.org/10.1109/ICEEE55327.2022.9772561.
[41] D. Bertsimas, D.B. Brown, C. Caramanis, Theory and applications of robust optimization, SIAM Rev. 53 (3) (2011) 464–501.
[42] C. Büsing, F. D'Andreagiovanni, New results about multi-band uncertainty in robust optimization, in: R. Klasing (Ed.), Experimental Algorithms, Springer, Berlin, Heidelberg, 2012, pp. 63–74.
[43] E. Isaksson, M. Karpe Conde, Solar power forecasting with machine learning techniques, 2018.
[44] P. Aupke, A. Kassler, A. Theocharis, M. Nilsson, M. Uelschen, Quantifying uncertainty for predicting renewable energy time series data using machine learning, Eng. Proc. 5 (1) (2021) 50.
[45] C.A. Ratanamahatana, E. Keogh, Making time-series classification more accurate using learned constraints, in: Proceedings of the 2004 SIAM International Conference on Data Mining, SIAM, 2004, pp. 11–22.
[46] G. Ke, Q. Meng, T. Finley, T. Wang, W. Chen, W. Ma, Q. Ye, T.-Y. Liu, Lightgbm: A highly efficient gradient boosting decision tree, Adv. Neural Inf. Process. Syst. 30 (2017).
[47] E. Al Daoud, Comparison between XGBoost, LightGBM and CatBoost using a home credit dataset, Int. J. Comput. Inf. Eng. 13 (1) (2019) 6–10.
[48] C. Chen, Q. Zhang, Q. Ma, B. Yu, LightGBM-PPI: Predicting protein-protein interactions through LightGBM with multi-information fusion, Chemometr. Intell. Lab. Syst. 191 (2019) 54–64.
[49] Y. Cao, L. Gui, Multi-step wind power forecasting model using LSTM networks, similar time series and lightgbm, in: 2018 5th International Conference on Systems and Informatics, ICSAI, IEEE, 2018, pp. 192–197.
[50] R. Koenker, K.F. Hallock, Quantile regression, J. Econ. Perspect. 15 (4) (2001) 143–156.
[51] W. Zhang, H. Quan, D. Srinivasan, Parallel and reliable probabilistic load forecasting via quantile regression forest and quantile determination, Energy 160 (2018) 810–819.